Genomic signatures of somatic hybrid vigor due to heterokaryosis in the oomycete pathogen, *Bremia lactucae*.

Kyle Fletcher [1]

Juliana Gil [1, 2]

Lien D Bertier [1]

Aubrey Kenefick [1]

Kelsey J Wood [1,3]

Lin Zhang [1]

Sebastian Reyes-Chin-Wo [1, 3, A]

Keri Cavanaugh [1]

Cayla Tsuchida [1, 2, B]

Joan Wong [1,3, C]

Richard Michelmore [1, 4, *]

*Corresponding author: rwmichelmore@ucdavis.edu

Affiliations:

[1] Genome Center, University of California, Davis, 95616, USA

[2] Plant Pathology Graduate Group, University of California, Davis, 95616, USA

[3] Integrated Genetics and Genomics Graduate Group, University of California, Davis, 95616, USA

[4] Departments of Plant Sciences, Molecular & Cellular Biology, Medical Microbiology & Immunology, University of California, Davis, 95616, USA

Current addresses:

[A] Bayer Crop Sciences, 37437 Ca-16 Woodland, CA, 95695

[B] Arcadia Biosciences, Davis, CA, 95616, USA

[C] Pacific Biosciences of California, Inc., Menlo Park, CA, 94025

Keywords

Heterokaryosis, oomycete, downy mildew, *Bremia lactucae*, genome sequence, comparative genomics, annotation, lettuce, virulence phenotype, effector repertoire

Abstract

Lettuce downy mildew caused by *Bremia lactucae* is the most important disease of lettuce globally. This oomycete pathogen is highly variable and has rapidly overcome resistance genes and fungicides deployed in attempts to control it. The described high-quality genome assembly of *B. lactucae* provides the foundation for detailed understanding of this economically important pathogen. The biotrophic nature of *B. lactucae* coupled with high levels of heterozygosity and the recently expanded repeat content made genome assembly challenging. The combined use of multiple read types, including synthetic long reads, single molecule sequences, and Hi-C, resulted in a high-quality, chromosome-scale, consensus assembly of this diploid organism. Phylogenetic analysis supports polyphyly in the downy mildews consistent with the biotrophic mode of pathogenesis evolving more than once in the Peronosporaceae. Flow cytometry plus resequencing of 30 field isolates as well as sexual offspring and asexual derivatives from multinucleate single sporangia demonstrated a high incidence of heterokaryosis in *B. lactucae*. Heterokaryons have phenotypic differences and increased fitness compared to homokaryotic derivatives. Consequently, *B. lactucae* exhibits somatic hybrid vigor and selection should be considered as acting on a population of nuclei within coenocytic mycelia. This provides evolutionary flexibility to the pathogen enabling rapid adaptation to different repertoires of host resistance genes and other challenges. The advantages of asexual persistence of heterokaryons may have been one of the drivers of selection that resulted in the loss of uninucleate zoospores in multiple downy mildews.

Oomycetes are genetically and biochemically distinct from fungi (*1, 2*) but have similar infection strategies and architectures. Oomycetes are successful diverse plant and animal pathogens with global economic impacts (*3-5*). These include the downy mildews caused by biotrophic members of the Peronosporaceae that are challenging to study due to their obligate reliance on their host. These pathogens are highly variable; plant resistance genes and fungicide treatments are often rapidly overcome (*6-12*). Various mechanisms have been proposed for rapid generation of genetic diversity including hyper-mutability of genomic regions that encode effectors (*13*), changes in ploidy (*14, 15*), and parasexuality (*16*).

Heterokaryosis, the state of having multiple genetically distinct nuclei in a single cell, is an important life history trait in some true fungi (*17, 18*). While transient heterokaryosis has been suggested and detected in oomycetes (*10, 15, 19-22*), the impacts of heterokaryosis remain poorly understood and rarely considered. The life cycles of many oomycetes are not conducive to the propagation of stable heterokaryons because they produce multiple flagellated, mono-nucleic, motile spores from sporangia (*21, 23*); heterokaryons are consequently broken every asexual generation (*21*). However, some downy mildew species including *Bremia lactucae* (*24*) do not produce zoospores and germinate directly from multinucleate sporangia (*25-31*), transmitting multiple, possibly genetically distinct nuclei in each asexual generation.

Bremia lactucae is an obligate biotroph that causes lettuce downy mildew, the most important disease of lettuce worldwide. Numerous races and population shifts have been documented in Europe, Australia, Brazil, and California (*32-38*). Resistance genes are rarely durable in the field and curative fungicides have become ineffective (*9-12*). Several mechanisms for variation have been documented. *B. lactucae* is predominantly heterothallic with two mating types and sexual reproduction can generate new virulence phenotypes (*39*). Asexual variation also occurs but is less well understood. Somatic fusion resulting in either polyploids or heterokaryons has been observed (*10, 20*), but it remained unclear if heterokaryosis or polyploidy are significant sources of stable

77 phenotypic variation of *B. lactucae*. Previously, sexual progeny of *B. lactucae* have been generated
78 to build genetic maps (*40, 41*), study genetics of (a)virulence and metalaxyl insensitivity (*9, 11, 42*),
79 and infer the presence of accessory chromosomes (*43*). Only limited genomic studies had been
80 conducted due to the difficulties of studying this biotrophic species (*44*).

81 This study presents a chromosome-scale genome assembly of *B. lactucae* using multiple
82 sequencing technologies and assembly approaches. This resource, combined with genome size
83 estimates generated by flow cytometry, was used to demonstrate the prevalence of heterokaryosis
84 in multiple *B. lactucae* isolates and the absence of polyploidy. Heterokaryons were shown to be
85 somatically stable and fitter on non-selective hosts compared to homokaryotic derivatives.
86 Homokaryotic components differed in (a)virulence phenotypes and conferred viability on selective
87 hosts. Selection should be considered as acting on a population of nuclei within a coenocytic
88 mycelium to maximize somatic hybrid vigor.

89 **Results and Discussion**

90 **Genome Assembly**

91 *Bremia lactucae* isolate SF5 was initially assembled into 885 scaffolds over 1 Kb with a contig
92 N_{50} of 30.6 Kb and a scaffold N_{50} of 283.7 Kb. The haploid genome size of this isolate and 38 others
93 were estimated to be ~152 Mb (+/- 3 Mb) by flow cytometry (Fig. 1a and Supplementary Table 1).
94 This 115 Mb assembly contained 91 Mb of sequence plus 24 Mb of gaps. Subsequently, 87.9 Mb
95 (96.5%) of the assembled sequence was placed into 22 scaffolds over 1 Mb using Hi-C; these totaled
96 112 Mb including gaps. The resultant assembly was highly collinear and comparable to the highly
97 contiguous v3.0 assembly of *Phytophthora sojae* (45), which cross-validates the high quality of both
98 assemblies (Fig. 1b). The heterozygosity of isolate SF5 was 1.17% and ranged from 0.77% to 1.29%
99 for other isolates. These levels ranked high compared to other oomycetes, the majority of which had
100 less than 1% heterozygosity (Fig. 1c). This level of heterozygosity resulted in some alleles not being

collapsed into a consensus sequence, necessitating multiple rounds of condensation to achieve a close to haploid consensus assembly.

The discrepancy between the final assembly size (91 Mb without gaps) and genome size measured by flow cytometry (152 Mb) is due to collapsed repeats in the assembly. Single-copy k-mers were present in the predicted proportions in the assembly; most of the homozygous k-mers and approximately half of the heterozygous k-mers were distributed across the two peaks as expected (Fig. 1d). BUSCO (*46*) analysis with the protist database (v9) also revealed 98.3% completeness similar to other well-assembled oomycetes (Table 1). Therefore, the assembly contains most of the single-copy portion of the genome. Repeat annotation followed by masking determined that 63 Mb of the 91 Mb assembled sequence was repetitive (Table 2). The majority of the annotated repeats were recently diverged long terminal repeat retrotransposons (LTR-RTs). Annotation identified 6.3 Mb as *Copia* (RLC) and 53.3 Mb as *Gypsy* (RLG) elements (Table 2). The average coverage of sequences annotated as repeats in the assembly was 2.1-fold higher than that of the annotated genes. Therefore, the 63-Mb repeat portion of the assembly is present at least twice in the haploid genome accounting for the 61 Mb difference between the assembly and the genome size determined by flow cytometry.

Divergence of LTR pairs showed that the majority of these repeat elements were recently expanded (Suppl. Mat. LTRplot), when compared to previously published downy mildews (Fig. 2b). The density of recently diverged LTRs was similar to that seen for *Phytophthora* spp. (Fig. 2a) although they were not as frequent. The larger genome assemblies of *S. graminicola* contained the largest number of annotated LTR-RTs of any downy mildew surveyed (Fig. 2b), although LTR pairs were more diverged than in *B. lactucae* (Fig. 2a). This suggests that the assemblies of *B. lactucae* and *Phytophthora* surveyed are of isolates which have undergone a recent expansion of *Copia* and *Gypsy* elements. Significantly, when LTR-RTs from each species were used to mask the assemblies, *B. lactucae* contained the highest proportion with 74.2% of its contig sequence masked (Fig. 2c).

Twenty-six to 46% of contig sequences were masked in most other species studied, except for the larger genomes of *S. graminicola* (two isolates) and *P. infestans* that had 72.1, 70.7, and 62.6% masked, respectively (Fig. 2 c). This high frequency of low-divergence repeat sequences in *B. lactucae* combined with its high heterozygosity (Fig. 1c) may have confounded assembly algorithms and slowed the generation of an accurate assembly as well as prevented the construction of whole chromosomal molecules. Interestingly, LTR divergence of *Plasmopara viticola*, which is a closer relative to *B. lactucae* than any *Phytophthora* spp. (Fig. 3; see below), does not have the same recent expansion of LTRs; this implies that this expansion of LTR-RTs was not ancestral to these species.

Phylogenomics

Phylogenetic analysis of 18 proteins identified with BUSCO supported polyphyly of downy mildew species within nine of the *Phytophthora* clades analyzed (Fig. 3). *B. lactucae* clustered with the two *Plasmopara* spp. and was most closely associated with *Phytophthora* clade 1, which includes *P. infestans* and *P. cactorum*. *B. lactucae* did not cluster with four other downy mildew species, *Peronospora effusa, Pseudoperonospora cubensis*, *Sclerospora graminicola*, and *Hyaloperonospora arabidopsidis*, which clustered closer to *P. agathidicida* in *Phytophthora* clade 5. Therefore, the biotrophic downy mildews evolved at least twice from hemi-biotrophic *Phytophthora*-like ancestors. This is consistent with previous, less extensive studies (*47-52*).

Gene Annotation

Ab initio annotation identified 9,781 protein-encoding genes. More than half (5,009) lacked introns, 1,949 had one intron, 1,063 had two introns, and 1,760 had three or more introns. A maximum of 20 introns was observed in two genes. The average gene length was 1,679 bp and ranged from 180 bp to 20.7 Kb. The mean exon length was 664 bp, ranging from 4 bp to 18.3 Kb, while the mean intron length was 104 bp, ranging from 10 bp to 9.3 Kb. The total gene space was 16.5 Mb, of which 15.2 Mb was exonic and 1.5 Mb was intronic. This is similar to other obligate biotrophic oomycetes, where the gene space ranges from 13.5 to 25.8 Mb. The hemi-biotrophic *P.*

sojae has the largest reported gene space within the Peronosporaceae at 37.7 Mb (Supplementary Table 2).

Motif searches revealed the repertoire of candidate effector proteins that could be important in pathogenesis. Among a total of 161 candidate secreted RxLR effectors, 66 had a canonical RxLR motif and 95 had degenerate [GHQ]xLR or RxL[GKQ] motifs (*44, 53, 54*); 64 candidates also encoded a [DE][DE][KR] motif (*55*) and/or a WY domain (*56, 57*) (Table 3). Expression inferred by presence in the transcriptome assembly was detected for 109 of these candidate RxLR effectors, 35 of which also had an EER motif or WY domain (Table 3). In addition to the 161 RxLR candidates, 26 predicted secreted proteins and 19 proteins lacking a secretion signal had one or more WY domains but no detectable RxLR motif. Of these, 19 WY proteins lacking an identifiable RxLR motif with a signal peptide and 13 without a signal peptide were detected in the transcriptome (Table 3). Interestingly, an EER or EER-like motif was detected in the first 100 residues from 29 of the 45 WY proteins that lacked an RxLR motif, 20 of which were predicted to be secreted. This is consistent with not all effectors requiring an RxLR motif for translocation in to the host cell, similar to previously reported effectors in animal pathogenic oomycetes (*58, 59*). Two putative secreted Crinklers (CRNs) (*60, 61*) were annotated, one of which also contained an RxLQ and DDR motif. An additional 74 CRNs lacking a secretion signal were identified, although only six of these were present in the transcriptome assembly (Table 3). Four of these six had the canonical LFLAK motif and the other two had a LYLA motif (*60, 61*). Together, these candidate effectors comprise 1.9% of all genes annotated in *B. lactucae*. Orthologs of all proteins which have previously been described as inducing a host response were detected in the draft assembly (Supplementary Table 3) (*62-64*). An additional 173 proteins (1.8% of all annotated genes) had domains ascribed to putative pathogenic functions in studies of other species (Supplementary Table 4). This is lower than the proportion reported for *Phytophthora* spp. (2.6 to 3.6%) and consistent with observations for other downy mildews where 1.3 to 1.7% of total annotated proteins had putative pathogenicity domains (*47*).

177 The majority of genes encoding flagella-associated proteins and calcium-associated domains
178 were missing from the *B. lactucae* genome. *B. lactucae* has lost 55 of 78 orthogroups that contain
179 flagellar proteins (Supplementary Fig. 2). One hundred and twelve proteins from *P. infestans* were
180 present in these orthogroups; 78 of these proteins were absent in *B. lactucae*. This is similar to
181 assemblies of other non-flagellate downy mildews that had 34 to 48 proteins in these orthogroups
182 (Supplementary Fig. 2). This is consistent with the loss of zoospore production by *B. lactucae*. There
183 was also a significant loss of calcium-associated domains, which is also observed in the assemblies of
184 other non-flagellate downy mildews. *B. lactucae* had no proteins present in 125 of the 177 calcium-
185 associated orthogroups similar to other non-flagellates, which ranged from 118 to 125. These
186 orthogroups contained 53 proteins from *B. lactucae* compared to 193 proteins in *P. infestans*. Other
187 non-flagellate species had 52 to 59 proteins assigned to these orthogroups (Supplementary Fig. 2).
188 The parallel loss of zoospore production and proteins with calcium-associated domains in both
189 clades of downy mildews (Fig. 3) is consistent with the involvement of these proteins in
190 zoosporegenesis (*65*). Genes encoding carbohydrate binding, transporter, and pathogenicity
191 associated domains were also under-represented in *B. lactucae* as previously reported for other
192 downy mildews in both clades (*47*). This provided further evidence for the convergent loss of genes
193 encoding these domains during adaptation to biotrophy.

194 The majority of annotated genes had levels of coverage close to the average sequencing
195 depth (Supplementary Fig. 3), indicating that most genes were each assembled into a single
196 consensus sequence. A minority of genes had a normalized read depth equal to half the sequencing
197 coverage, consistent with divergent haplotypes that had assembled as independent sequences. The
198 BUSCO (*46*) genes had the same distribution. However, genes encoding candidate effectors had
199 variable coverage; this could have been due to a disproportionate number of effector haplotypes
200 being assembled independently and/or a high rate of divergence between haplotypes resulting in
201 poor mapping rates.

Genomic signatures of heterokaryosis

Distinct alternative allele frequency profiles were detected in multiple isolates of *B. lactucae* (Fig. 4 and Supplementary Fig. 4). Such analysis had previously been used to support polyploidy in *P. infestans* (*14, 66*). The profiles of thirteen isolates, including the reference isolate SF5, were clearly unimodal, seven isolates were trimodal, and nine isolates were trimodal (Supplementary Fig. 4). Two other isolates had profiles that were not clearly bimodal or trimodal (Supplementary Fig. 4). The symmetrical unimodal distribution of SF5 was consistent with a diploid genome; the other distributions were not. However, the genome size for all isolates as measured by flow cytometry varied by less than 3%. In the case of polyploidy, the genome size of triploids and tetraploids would be 150% and 200% that of the diploid, respectively; therefore, there was no evidence for polyploidy in *B. lactucae* (Fig. 1 a and Supplementary Table 1).

Further evidence against polyploidy was provided by analysis of sexual progeny from the segregating F_1 population of SF5 (unimodal) x California isolate C82P24 (trimodal; Fig. 4b) (*20, 40*). Four progeny isolates sequenced to over 50x all had unimodal allele frequency plots (Supplementary Fig. 5). Flow cytometry of 16 progeny isolates had the same genome sizes as all other isolates (Fig. 1a and Supplementary Table 1). The outcross origin of these progeny was confirmed by the presence of unique combinations of SNPs inherited from each parent. Therefore, these progeny isolates could not have arisen by apomixis or selfing and all sexual progeny from this unimodal x trimodal cross were diploid. The origins of the gametes in this cross were determined for 38 progeny isolates that had been sequenced to sufficient depth. Pairwise SNP-based kinship coefficients revealed two distinct half-sib families of 29 and 9 individuals (Fig. 5). Therefore, three rather than two nuclei contributed gametes in this cross. The trimodal alternative allele frequency plot and flow cytometry of C82P24 are consistent with this isolate being heterokaryotic with two diploid nuclei.

To confirm that C82P24 was heterokaryotic rather than a mixture of two isolates, 20 asexual derivatives were generated from single sporangia. Kinship of these 20 isolates was as high between

one another as with the original isolate, indicating they were identical. Furthermore, all asexual derivatives of C82P24 displayed similar relatedness to all sexual progeny (Fig. 5). Sequencing of 11 asexual derivatives to >50x coverage demonstrated that they retained the trimodal profile, indicating that two distinct nuclei were present in each derivative (Supplementary Fig. 6) with a diploid size of 303 +/- 3 Mb as measured by flow cytometry (Supplementary Table 5). Therefore, C82P24 was heterokaryotic rather than a mixture of isolates.

To demonstrate heterokaryosis in another isolate, 10 asexual derivatives were also generated from isolate C98O622b, which displayed a trimodal alternative allele frequency. In this case, kinship analysis revealed three distinct groups of derivatives (Fig. 6i). Derivatives A to F had a high kinship and an identical virulence phenotype to C98O622b (Fig. 6i, ii). Derivatives G to I and derivative J had lower kinship to C98O622b than derivatives A to F. The lowest kinship was between derivatives G to I and J (Fig. 6i). Virulence phenotypes varied between but not within groups (Fig. 6ii); C98O622b and derivatives A to F were virulent on both *Dm4* and *Dm15*; derivatives G to I were avirulent on *Dm4* and virulent on *Dm15*, while derivative J was conversely virulent on *Dm4* and avirulent on *Dm15* (Fig. 6ii). The single-spore derivatives of C98O622b were sequenced to >50x coverage to determine their nuclear composition. Derivatives A to F were trimodal (Fig. 5iii, Supplementary Fig. 7); all other derivatives were unimodal, which is consistent with the separation of the heterokaryon into its diploid components (Fig. 6iii). This conclusion was supported by combining read sets *in silico*. Combining reads of derivatives G-I did not increase their relatedness to C98O622b, while combining reads of derivatives G, H, or I with those of J resulted in a high kinship to C98O622b (Fig. 6i) and trimodal profile similar to C98O622b (Fig. 6iii and Supplementary Fig. 8). Therefore, C98O622b was also heterokaryotic; however, unlike C82P24, C98O622b was unstable and could be separated into constituent homokaryotic derivatives by sub-culturing from single sporangia.

The trimodal distributions of the derivatives A to F were not identical and could clearly be split into two configurations. Derivatives B and F were similar to C98O622b, displaying peaks at approximately 0.25, 0.5, and 0.75 (Fig. 6iii). The other four heterokaryotic derivatives A, C, D, and E had peaks at approximately 0.33, 0.5, and 0.67 (Fig. 6iii). The nuclear composition of these heterokaryotic derivatives was investigated by subsampling SNPs identified as unique to each homokaryotic derivative (G to J). This revealed that in the trimodal distribution of derivatives B and F (0.25, 0.5, 0.75) SNPs unique to either constituent nucleus were in peaks at 0.25 and 0.75 (Fig. 6iv, Supplementary Fig. 9), consistent with a balanced 1:1 ratio of constituent nuclei (1:3 read ratio of SNPs). For derivatives A, C, D, and E (peaks at 0.33, 0.5, 0.67), SNPs unique to constituent nuclei resembling derivatives G to I were consistently in peaks at approximately 0.17 and 0.83, while SNPs identified as unique to derivative J were consistently in peaks at 0.33 and 0.67 (Fig. 6iv, Supplementary Fig. 9), consistent with a 2:1 unbalanced nuclear ratio in favor of nuclei similar to derivative J. This was further supported by combining reads *in silico*. Combining reads from derivatives G, H, or I with J in equal proportions resulted in trimodal plots similar to those of derivatives B and F (peaks at 0.25, 0.5, and 0.75; Supplementary Fig. 8). Combining reads from derivatives G, H, or I with J in a ratio of 1:2 resulted in frequency profiles like those of derivatives A, C, D, and E (peaks at 0.33, 0.5, and 0.67; Supplementary Fig. 8). This supports an unequal nuclear composition in four of the asexual derivatives of C98O622b.

Somatic hybrid vigor due to heterokaryosis

To investigate the potential benefits of heterokaryosis, the fitness of asexual derivatives of C98O622b was assessed on a universally susceptible cultivar and two differential host lines. Derivatives A and B were selected to represent unbalanced and balanced heterokaryons, respectively, while derivatives I and J represented the two homokaryons. When grown on the universally susceptible lettuce cv. Green Towers, the heterokaryotic derivatives grew faster than either homokaryotic derivative. The balanced heterokaryotic derivative B was significantly fitter than

276 the homokaryotic derivative I (Fig. 7 a). There was no significant difference within heterokaryotic
277 derivatives or within homokaryotic derivatives when grown on cv. Green Towers. Therefore, the
278 heterokaryotic isolates were fitter when unchallenged by host resistance genes. However, when a
279 product of either nucleus of the heterokaryon was detected by a resistance gene (i.e. *Dm4* in
280 R4T57D or *Dm15* in NumDM15) that differentiates the homokaryotic derivatives (Fig. 6 ii), the
281 heterokaryotic derivatives were less vigorous than the virulent homokaryotic derivative (Fig. 7 b).
282 This suggested that it may be possible to break a heterokaryon by repeated subculture on a selective
283 cultivar, as reported previously (*10*). When the heterokaryotic derivatives were inoculated onto an F_1
284 hybrid of the selective lines expressing both *Dm4* and *Dm15*, neither the heterokaryotic nor
285 homokaryotic derivatives were able to grow. Therefore, combining multiple resistance genes against
286 the entire *B. lactucae* population into a single cultivar remains a potentially effective strategy to
287 provide more durable resistance to the pathogen.

288 Heterokaryosis in *B. lactucae* has phenotypic consequences as well as implications for
289 interpretation of tests for virulence phenotype. Derivatives G, H, and I are race Bl:5-CA and
290 derivative J has a novel virulence phenotype. The heterokaryotic field isolate C98O622b is race Bl:6-
291 CA, indicating that two phenotypically distinct isolates may combine to create a new phenotype
292 when characterized on individual resistance genes; such somatic hybrids may not be able to
293 overcome combinations of these resistance genes in a single cultivar. Therefore, reactions of
294 monogenic differentials are not necessarily a good predictor of virulence when heterokaryons are
295 tested. The instability of heterokaryosis may enable a successful infection and proliferation of
296 individual nuclear components. Furthermore, there is no *a priori* reason why coenocytic mycelia are
297 limited to having only two nuclear types. Multiple rounds of somatic fusion are possible if favored by
298 selection. Allele frequency plots are consistent with some isolates having more than two nuclei (e.g.
299 isolate C04O1017; Fig. 4 c). Therefore, heterokaryotic isolates should be considered as exhibiting
300 somatic hybrid vigor and selection for heterosis in *B. lactucae* as acting on populations of nuclei
301 within a coenocytic mycelium (Fig. 8) rather than on individual isolates.

Heterokaryosis in other oomycetes

Heterokaryosis may be a common phenomenon in other oomycetes that has yet to be investigated extensively. Flow cytometry revealed heterogeneous nuclear sizes in mycelia of *P. infestans*, although stability over multiple asexual generations was not reported (*19*). Somatic fusion may be a route to allopolyploidy; inter-species somatic fusion could result in transient heterokaryosis before nuclear fusion to form a somatic allopolyploid circumventing gametic incompatibility. Somatic sporangial fusions have also been reported in a "basal" holocarpic oomycete (*67*) demonstrating the possibility of widespread heterokaryosis within the family. Heterokaryosis may be more prevalent in non-zoospore producing oomycetes. Production of zoospores with single nuclei during the asexual cycle, exhibited by many oomycetes breaks the heterokaryotic state each asexual generation (*21, 23*). However, some downy mildews and *Phytophthora* spp. germinate directly from multinucleate sporangia, which potentially maintains the heterokaryotic state, as shown in our data. The increased fitness and phenotypic plasticity of heterokaryosis could be one of the selective forces favoring the loss of zoospore genesis in multiple lineages of oomycete pathogens (*24, 47*).

Heterokaryosis should be considered when implementing strategies for deployment of resistance genes. Cycles of somatic fusion to increase fitness and selection on populations of nuclei provide potentially great phenotypic plasticity without mutation. This could result in rapid changes in pathogen populations in response to changes in host genotypes or fungicide use. Comprehensive knowledge of the prevalence and virulence phenotypes of homokaryotic and heterokaryotic isolates as well as the population dynamics are necessary to predict the evolutionary potential of a pathogen population.

Methods

Isolation, culturing, and DNA extraction

Bremia lactucae isolate SF5 has been reported previously (*20, 40, 41*). Additional field isolates surveyed in this study were either isolates collected from California/Arizona between 1982 and 2015 or were supplied by Diederik Smilde (Naktuinbouw, The Netherlands). Sexual progeny of SF5 x C82P24 were generated as described previously (*40, 41*). Single-spore isolates were derived from cotyledons that had been sporulating asexually for 1 to 2 days (6 to 7 days post-infection). A single cotyledon was run over a 0.5% water agar plate until clean of spores. Single conidia were located under a dissection microscope, pulled off the agar using pipette tips, and ejected onto fresh, 7-day old cotyledons of cv. Green Towers that had been wetted with a drop of deionized water. Plates were incubated at 15˚C with 12 hour light/dark periods. Successful single-spore infections were transferred to cv. Green Towers seedlings and maintained thereon. Fitness was determined by measuring the rate of *B. lactucae* sporulation of four replicates of four isolates on 20 cotyledons at 3, 5, 6, 7, and 9 days post-inoculation (dpi) on cv. Green Towers. The area under the curve was calculated for each replicate and significance tested using a two-tailed t-test with Holm adjustment. Additional fitness tests of heterokaryons were performed on an F_1 hybrid of NumDm15 and R4T57D, which confer resistance phenotypes Dm15 and Dm4, respectively (*68*). The virulence phenotype was determined by inoculation onto the IBEB EU-B standardized differential set (http://www.worldseed.org/wp-content/uploads/2016/05/Table-1_IBEB.pdf) and observed for sporulation at 7, 11, 15, and 21 dpi. Microscopy was performed on ~2-week old seedlings of lettuce cv. Green Towers, 5 dpi with *B. lactucae* isolate C16C1909 (Fig. 8a) or ~2 week old seedlings of lettuce cv. Cobham Green homozygous for the AtUBI::dsRED transgene, 7 dpi with *B. lactucae* isolate C98O622b (Fig. 8b). Fig. 8a was captured with a Leica TCS SP8 STED 3X inverted confocal microscope using a 40x water immersion objective. Image processing was performed using Huygens Professional (https://svi.nl/Huygens-Professional) and Bitplane Imaris (http://www.bitplane.com/). Fig. 8b was captured using a Zeiss LSM 710 laser scanning confocal microscope using a 40x water immersion objective. Z stacks were processed and combined into a single image using the ZEN Black software.

Spore pellets of all isolates sequenced were obtained by washing sporangia from infected lettuce cotyledons in sterile water. Spore suspensions were concentrated by centrifugation in 15 mL tubes, resuspended, transferred to microfuge tubes, pelleted, and stored at -80°C until DNA extraction following a modified CTAB procedure (*69*). Quantity and quality of DNA was determined by spectrometry as well as estimated by TAE gel electrophoresis.

Library preparation and sequencing

Paired-end (300 bp fragments) and mate-pair (2-, 5-, 7-, and 9-Kb) libraries were prepared using Illumina (San Diego, CA), NEB (Ipswich, MA), and Enzymatic (Beverly, MA) reagents following the manufacturers' protocols. RNAseq libraries were constructed from cotyledons of cv. Cobham Green infected with isolate SF5 following the protocol by Zhong *et al.* (*70*), except that the mRNA was not fragmented and instead the cDNA was sonicated with a Covaris S220 following the manufacturer's recommendations to achieve 150-bp fragments before end repair. Size selection and purification were performed after adaptor ligation using 0.8x Agencourt Ampure beads XP (Beckman Coulter, Brea, CA). Synthetic long reads were generated by Moleculo (now Illumina) from barcoded libraries. Libraries were sequenced by the DNA Technologies Core at the UC Davis Genome Center (http://genomecenter.ucdavis.edu) on either a Hiseq 2500 or 4000.

The random-shear BAC library was constructed by Lucigen Corporation (Middleton, WI); this provided 10,000 BAC clones with a mean insert size of 100 kb. Sanger sequencing of BAC ends was performed by the Genome Institute at Washington University (St. Louis, MO) and generated sequences averaging 700 bp in length. A fosmid library consisting of over eight million clones with a mean insert size of 40 kb was generated by Lucigen Corporation and end-sequenced on an Illumina MiSeq. Two SMRTbell™ libraries with mean insert sizes of 3 kb and 10 kb were constructed and sequenced by Pacific Biosciences. Hi-C libraries were produced by Dovetail Genomics.

Flow cytometry

Flow cytometry of select isolates was performed on sporulating cotyledons 7 dpi. For each measurement, two sporulating cotyledons were mixed with 1 cm^2 of young leaf tissue from *Oryza sativa* cv. Kitaake (2C = 867 Mb), which was sufficiently different from the genome size of *B. lactucae* (2C and 4C) for use as the internal reference. The *O. sativa* 2C DNA content was determined by calibrating against nuclei from flower buds of *Arabidopsis thaliana* Col-0, which has a known absolute DNA content of 2C = 314 Mb (*71*). Nuclei extraction and staining with propidium iodide was done using the Cystain PI absolute P kit (Sysmex, Lincolnshire, IL). Flow cytometry was done on a BD FACScan (Becton Dickinson, East Rutherford, NJ). For each measurement, 10,000 nuclei were assessed, and each isolate was measured three times. Lettuce nuclei are ~3x larger than rice nuclei and did not interfere with the measurements. Data was analyzed using FlowJo (Ashland, OR). Total nuclear DNA content was averaged over all replicates. Means and standard deviations were calculated from the average nuclear content of each isolate. Haploid genome size was calculated by halving the mean across all isolates.

De novo assembly, assessment, and annotation

Multiple assembly approaches were tried using a variety of templates. Ultimately, the genome of isolate SF5 was assembled using a hybrid approach using several types of sequences (Supplementary Fig. 10). Moleculo reads were assembled using Celera (*72*) and further scaffolded using mate-pair, fosmid-end, BAC-end, and PacBio data utilizing first SSPACE v3.0 (*73*) followed by AHA (*74*). A consensus assembly was obtained by removing the second haplotype using Haplomerger2 (*75*). Misjoins were detected and broken using REAPR v1.0.18 in 'aggressive mode' (*76*). Mitochondrial sequences were detected by BLASTn v 2.2.28 and removed before final scaffolding and gap-filling (*73, 77*). Hi-C scaffolding was performed by Dovetail Genomics using their Hi-Rise pipeline to infer breaks and joins. One putative effector gene was masked by Ns in the assembly because it was determined by read coverage to be erroneously duplicated multiple times.

The quality of the assembly was assessed in multiple ways. Assembly completeness and duplication was measured by BUSCO v2, protist ensemble library db9 (*46*) and KAT v2.4.1 (*78*). Nucleotide colinearity between *B. lactucae* and *Phytophthora sojae* was inferred using Promer v3.06 (-l 30) and visualized using Symap v4.2 (*79*) set with a required minimum of 5 dots. Phylogenetic analysis was performed on amino acid sequences of single-copy proteins predicted by BUSCO; 18 sequences from *B. lactucae* that were also present in assemblies of all 20 *Phytophthora* spp., *Plasmopara* spp., *H. arabidopsidis*, *S. graminicola*, *Pseudoperonospora cubensis*, and *P. effusa* were aligned independently with MAFFT v7.245 (*80*), concatenated into single sequences for each species/isolate, and phylogenetically tested with RAxML v8.0.26, run with 1,000 bootstraps (*81*).

A *de novo* transcriptome assembly was generated by mapping reads with BWA MEM v0.7.12 (*82*) to a combined reference of the *B. lactucae de novo* assembly and *L. sativa* assembly (*83*). Reads that mapped to the *B. lactucae* assembly were assembled with Trinity v2.2.0 (*84*) and filtered with BLAST to ensure that the transcripts belonged to *B. lactucae*. Transcripts were translated with Transdecoder v3.0.0 (*85*).

Primary annotation was performed using MAKER v2.31.8 (*86*). The RNAseq assembly was first used to predict proteins from the SF5 genome with no HMMs. These models were then filtered and used to produce HMMs with SNAP v2006-07-28 (*87*), which in turn were used with MAKER for *ab initio* gene model predictions. Additional candidate effectors were predicted through regular expression string searches (RxLR & EER) and HMMs (WY & CRN) as previously described (*47*). A previously published RxLR-EER HMM (*88*) was also applied, though it failed to define additional candidate effectors compared to regular expression string searches. These gene models were filtered and prepared for submission to NCBI using GAG v2.0-rc.1 (*89*). Transcriptional support for putative effectors was inferred by >=95% tBLASTn identity and <$1e^{-75}$ e-value scored between the protein and the transcript. Absence of genes encoding domains linked to zoosporogenesis and biotrophy was performed as previously described (*47*). Coverage of gene models was calculated with

BEDtools2 v2.25.0 multicov (*90*), multiplying the result by the read length (101 bp), and dividing by the length of the gene. Comparative annotation analysis was undertaken by downloading GFF files of all annotated oomycetes from FungiDB (*91*) and using GAG (*89*) to obtain summary statistics of annotations.

Repeat analysis

Repeat libraries were produced independently from RepeatModeler v1.0.8 (*92*) and a LTRharvest v1.5.7 / LTRdigest v1.5.7 (*93, 94*) pipeline adapted from that previously used on *P. tabacina* and *P. effusa* (*47, 95*). Briefly, provisional LTRs were identified as being separated by 1 to 40 kb with LTRharvest. LTRdigest was used to identify complete LTR-RTs that were then annotated by similarity to elements in TREP. Elements containing sequences annotated as genes were removed. These libraries were combined and run through RepeatMasker v4.0.6 (*96*). Coverage of each non-overlapping masked repeat region was calculated with BEDTools2 v2.25.0 multicov (*90*) using the coordinates of the repeat elements and the BAM file generated by mapping SF5 reads back to the assembly with BWA-MEM v0.7.12 (*82*).

Divergence of LTRs for *B. lactucae* and additional oomycete assemblies was calculated in a similar manner to that previously reported (*95*). LTRharvest (*93*) and LTRdigest (*94*) were run as above. Internal domains of annotated LTR-RTs were clustered with VMatch, followed by alignment of 3' and 5' LTRs with Clustal-O (*97*). Too few internal domains were detected for *P. halstedii* to allow clustering, so it was excluded from this analysis. Divergence between aligned 3' and 5' LTRs was calculated with BaseML and PAML (*98*) and plotted using R base packages (*99*). Divergence between LTR pairs calculated for each species are provided (Supplementary Table 6). LTR frequency and percentage of the genome of each species/isolate masked was plotted with ggplot2 (*100*) (Supplementary Table 7). These predictions were not filtered for overlaps with gene annotations as multiple genomes analyzed do not have publicly available annotations (Supplementary Table 2).

Analyses of additional read sets

Whole-genome sequencing data of additional oomycetes were downloaded from NCBI SRA (Supplementary Table 8) and converted to fastq files using the SRA-toolkit (*101*). Heterozygosity was calculated by generating 21-mer histograms with JELLYFISH v2.2.7 (*102*) and plotted with GenomeScope (*103*). Isolates that did not fit a diploid model were excluded from the analysis.

Paired-end reads of all sequenced *B. lactucae* isolates were trimmed and adapter-filtered using BBMap (*104*), filtered for reads of a bacterial origin by mapping to a database of all bacteria genome sequences on NCBI, and mapped to the final reference assembly of SF5 using BWA MEM v0.7.12 (*82*). Alternative allele frequency plots were generated as described previously (*14, 66*) for all isolates sequenced to over 50x using SAMtools mpileup v0.1.18 (*105*) with a quality flag of 25 to perform individual pileups on each BAM file, followed by BCFtools v0.1.19 (*106*) to convert to human-readable format. Bash was used to parse the files and generate the frequency of the alternative allele for every SNP that was covered by >50 reads and had an allele frequency between 0.2 to 0.8. In some instances, this frequency filter was removed to investigate the full spectrum of peaks. Bar charts were plotted with the R base package (*99*). Intersections of SNPs common to heterokaryotic and homokaryotic derivatives were obtained with BEDTools2 v2.25.0 intersect (*90*).

Kinship analysis was performed on progeny and derivatives sequenced to a depth greater than 10x. Reads were trimmed, filtered, and mapped as above. Multi-sample pileups were obtained with SAMtools mplileup v0.1.18 (*105*) and made human readable using BCFtools v0.1.19 (*106*), and pairwise kinship was calculated using VCFtools v0.1.14 with the relatedness2 flag (*107, 108*). The two-column table output was transformed into a matrix using bash, and conditional formatting was used to visualize relationships. Raw matrices of these analyses are available (Supplementary Table 9 & 10).

Acknowledgements

We thank Melodie Najarro (UC Davis) for preparing *B. lactucae* cultures and Dave Tricoli for the transgenic DsRED lettuce line used for microscopy. We thank D. Smilde for supplying European (BL) isolates for sequencing. We thank Dovetail for Hi-C analysis and Dr. C.-C. Wu at Lucigen for construction of the BAC library and the staff of the DNA Technologies Core of the UC Davis Genome Center for their sequencing efforts. We thank staff of the UC Davis Flow Cytometry Core for technical assistance. The work was supported by the NSF/USDA Microbial Sequencing Program award # 2009-65109-05925 and the Novozymes Inc. Endowed Chair in Genomics to RWM.

Author contributions:

KF performed the assembly, annotation, and inter- and intra-comparative genomics as well as drafted the manuscript. RJG performed phenotyping of isolates, culturing, generation of the genetic cross, and DNA and RNA extractions. LB performed flow cytometry and confocal microscopy. AK performed culturing, DNA extractions, phenotyping of isolates, and obtained asexual single spore derivatives. KW prepared the qPCR investigation. LZ, KC, and JW performed culturing and DNA extractions. SR generated the first assembly. CT performed culturing, phenotyping of isolates, generation of the genetic cross, and DNA extractions. RM supervised and conceptualized the project and made significant contributions to all drafts. All authors contributed to the final manuscript and approved the submission.

Competing interests: The authors declare no competing interests.

Data availability: All sequence data are available at NCBI under BioProjects ##########., ##########., ##########., and ##########.

Code/Software availability: All software is described and cited in the article. A workflow summary of the assembly is provided (Supplementary Figure 10a)

References

1. S. L. Baldauf, A. J. Roger, I. Wenk-Siefert, W. F. Doolittle, A kingdom-level phylogeny of eukaryotes based on combined protein data. *Science (New York, N.Y.)* **290**, 972-977 (2000).
2. M. L. Sogin, J. D. Silberman, Evolution of the protists and protistan parasites from the perspective of molecular systematics. *International journal for parasitology* **28**, 11-20 (1998).
3. I. R. Crute. (Prentice Hall, Inc., Englewood Cliffs, New Jersey, 1992), pp. 165-185.
4. F. P. Meyer, Aquaculture disease and health management. *Journal of animal science* **69**, 4201-4208 (1991).
5. A. J. Haverkort *et al.*, Societal Costs of Late Blight in Potato and Prospects of Durable Resistance Through Cisgenic Modification. *Potato Research* **51**, 47-57 (2008).
6. S. Zhu, Y. Li, J. H. Vossen, R. G. F. Visser, E. Jacobsen, Functional stacking of three resistance genes against Phytophthora infestans in potato. *Transgenic Research* **21**, 89-99 (2012).
7. A. Saville *et al.*, Fungicide Sensitivity of U.S. Genotypes of Phytophthora infestans to Six Oomycete-Targeted Compounds. *Plant Disease* **99**, 659-666 (2014).
8. R. Childers *et al.*, Acquired Resistance to Mefenoxam in Sensitive Isolates of Phytophthora infestans. *Phytopathology* **105**, 342-349 (2014).
9. I. R. CRUTE, J. M. HARRISON, Studies on the inheritance of resistance to metalaxyl in Bremia lactucae and on the stability and fitness of field isolates. *Plant Pathology* **37**, 231-250 (1988).
10. T. Schettini, E. Legg, R. Michelmore, Insensitivity to metalaxyl in California populations of Bremia lactucae and resistance of California lettuce cultivars to downy mildew. *Phytopathology* **81**, 64-70 (1991).
11. I. Crute, The occurrence, characteristics, distribution, genetics, and control of a metalaxyl-resistant pathotype of Bremia lactucae in the United Kingdom. *Plant disease (USA)*, (1987).
12. T. Ilott, M. Durgan, R. Michelmore, Genetics of virulence in Californian populations of Bremia lactucae(lettuce downy mildew). *Phytopathology* **77**, 1381-1386 (1987).
13. S. Dong, S. Raffaele, S. Kamoun, The two-speed genomes of filamentous pathogens: waltz with plants. *Current opinion in genetics & development* **35**, 57-65 (2015).
14. Y. Li *et al.*, Changing Ploidy as a Strategy: The Irish Potato Famine Pathogen Shifts Ploidy in Relation to Its Sexuality. *Molecular Plant-Microbe Interactions* **30**, 45-52 (2016).
15. L. Bertier, L. Leus, L. D'hondt, A. W. A. M. de Cock, M. Höfte, Host Adaptation and Speciation through Hybridization and Polyploidy in Phytophthora. *PLOS ONE* **8**, e85385 (2013).
16. O. Spring, R. Zipper, Asexual Recombinants of Plasmopara halstedii Pathotypes from Dual Infection of Sunflower. *PLOS ONE* **11**, e0167015 (2016).
17. N. B. Strom, K. E. Bushley, Two genomes are better than one: history, genetics, and biotechnological applications of fungal heterokaryons. *Fungal Biology and Biotechnology* **3**, 4 (2016).
18. J. F. Leslie, Fungal vegetative compatibility. *Annu Rev Phytopathol* **31**, (1993).
19. M. Catal *et al.*, Heterokaryotic nuclear conditions and a heterogeneous nuclear population are observed by flow cytometry in Phytophthora infestans. *Cytometry. Part A : the journal of the International Society for Analytical Cytology* **77**, 769-775 (2010).
20. S. Hulbert, R. Michelmore, DNA restriction fragment length polymorphism and somatic variation in the lettuce downy mildew fungus, Bremia lactucae. *Molecular plant-microbe interactions: MPMI (USA)*, (1988).
21. M. Long, N. Keen, Evidence for heterokaryosis in Phytophthora megasperma var. sojae. *Phytopathology* **67**, 4 (1977).
22. R. Michelmore, D. Ingram, Secondary homothallism in Bremia lactucae. *Transactions of the British Mycological Society* **78**, 1-9 (1982).
23. C. A. Walker, P. van West, Zoospore development in the oomycetes. *Fungal Biology Reviews* **21**, 10-18 (2007).
24. H. S. Judelson, J. Shrivastava, J. Manson, Decay of genes encoding the oomycete flagellar proteome in the downy mildew Hyaloperonospora arabidopsidis. *PloS one* **7**, e47624 (2012).

25. Y. Cohen, U. Gisi, T. Niderman, Local and systemic protection against Phytophthora infestans induced in potato and tomato plants by jasmonic acid and jasmonic methyl ester. *Phytopathology* **83**, 1054-1062 (1993).
26. D. Glendinning, J. A. Macdonald, J. Grainger, Factors affecting the germination of sporangia in Phytophthora infestans. *Transactions of the British Mycological Society* **46**, 595-603 (1963).
27. D. E. Hemmes, H. R. Hohl, Ultrastructural Changes in Directly Germinating Sporangia of Phytophthora parasitica. *American Journal of Botany*, 300-313 (1969).
28. P. van West, A. A. Appiah, N. A. R. Gow, Advances in research on oomycete root pathogens. *Physiological and Molecular Plant Pathology* **62**, 99-113 (2003).
29. L. J. Grenville‐Briggs, P. v. West, in *Advances in Applied Microbiology*. (Academic Press, 2005), vol. Volume 57, pp. 217-243.
30. H. S. Judelson, F. A. Blanco, The spores of Phytophthora: weapons of the plant destroyer. *Nature Reviews Microbiology* **3**, 47-58 (2005).
31. L. Willoughby, Pure culture studies on the aquatic phycomycete, Lagenidium giganteum. *Transactions of the British Mycological Society* **52**, 393IN393-410IN396 (1969).
32. R. Castoldi *et al.*, Identification of new Bremia lactucae races in lettuce in São Paulo state. *Horticultura Brasileira* **30**, 209-213 (2012).
33. D. S. Trimboli, J. Nieuwenhuis, New races of Bremia lactucae on lettuce in Australia. *Australasian Plant Disease Notes* **6**, 62-63 (2011).
34. K. v. Ettekoven, A. van Arend, in *Eucarpia Leafy Vegetables' 99, Olomouc (Czech Republic), 8-11 Jun 1999*. (Palacky University, 1999).
35. I. R. Crute, A. G. Johnson, The genetic relationship between races of Bremiae lactucae and cultivars of Lactuca sativa. *Annals of Applied Biology* **83**, 125-137 (1976).
36. I. Petrželová, A. Lebeda, E. Kosman, Distribution, disease level and virulence variation of Bremia lactucae on Lactuca sativa in the Czech Republic in the period 1999–2011. *Journal of Phytopathology* **161**, 503-514 (2013).
37. A. Lebeda, I. Petrželová, Variation and distribution of virulence phenotypes of Bremia lactucae in natural populations of Lactuca serriola. *Plant Pathology* **53**, 316-324 (2004).
38. A. Lebeda, V. Zinkernagel, Evolution and distribution of virulence in the German population of Bremia lactucae. *Plant Pathology* **52**, 41-51 (2003).
39. R. W. Michelmore, D. S. Ingram, Heterothallism in Bremia lactucae. *Transactions of the British Mycological Society* **75**, 47-56 (1980).
40. D. Sicard *et al.*, A genetic map of the lettuce downy mildew pathogen, Bremia lactucae, constructed from molecular markers and avirulence genes. *Fungal Genet Biol* **39**, 16-30 (2003).
41. S. H. Hulbert *et al.*, Genetic analysis of the fungus, Bremia lactucae, using restriction fragment length polymorphisms. *Genetics* **120**, 947-958 (1988).
42. J. M. Norwood, R. W. Michelmore, I. R. Crute, D. S. Ingram, The inheritance of specific virulence in Bremia lactucae (downy mildew) to match resistance factors 1, 2, 4, 6 and 11 in Lactuca sativa (lettuce). *Plant Pathology* **32**, 177-186 (1983).
43. D. M. Francis, R. W. Michelmore, Two classes of chromosome-sized molecules are present in Bremia lactucae. *Experimental Mycology* **17**, 284-300 (1993).
44. J. H. Stassen *et al.*, Effector identification in the lettuce downy mildew Bremia lactucae by massively parallel transcriptome sequencing. *Mol Plant Pathol* **13**, 719-731 (2012).
45. B. M. Tyler *et al.*, Phytophthora genome sequences uncover evolutionary origins and mechanisms of pathogenesis. *Science (New York, N.Y.)* **313**, (2006).
46. F. A. Simao, R. M. Waterhouse, P. Ioannidis, E. V. Kriventseva, E. M. Zdobnov, BUSCO: assessing genome assembly and annotation completeness with single-copy orthologs. *Bioinformatics* **31**, 3210-3212 (2015).

47. K. Fletcher *et al.*, Comparative genomics of downy mildews reveals potential adaptations to biotrophy. *BMC Genomics*, (in press).
48. R. Sharma *et al.*, Genome analyses of the sunflower pathogen Plasmopara halstedii provide insights into effector evolution in downy mildews and Phytophthora. *BMC Genomics* **16**, 741 (2015).
49. A. Riethmuller, H. Voglmayr, M. Goker, M. Weiß, F. Oberwinkler, Phylogenetic relationships of the downy mildews (Peronosporales) and related groups based on nuclear large subunit ribosomal DNA sequences. *Mycologia* **94**, 834-849 (2002).
50. C. G. P. McCarthy, D. A. Fitzpatrick, Phylogenomic Reconstruction of the Oomycete Phylogeny Derived from 37 Genomes. *mSphere* **2**, (2017).
51. M. Thines *et al.*, Phylogenetic relationships of graminicolous downy mildews based on cox2 sequence data. *Mycological Research* **112**, 345-351 (2008).
52. T. B. Bourret *et al.*, Multiple origins of downy mildews and mito-nuclear discordance within the paraphyletic genus Phytophthora. *PLOS ONE* **13**, e0192502 (2018).
53. R. G. Anderson, D. Deb, K. Fedkenheuer, J. M. McDowell, Recent Progress in RXLR Effector Research. *Mol Plant Microbe Interact* **28**, 1063-1072 (2015).
54. P. Mestre *et al.*, Comparative analysis of expressed CRN and RXLR effectors from two Plasmopara species causing grapevine and sunflower downy mildew. *Plant Pathology* **65**, 767-781 (2016).
55. B. J. Haas *et al.*, Genome sequence and analysis of the Irish potato famine pathogen Phytophthora infestans. *Nature* **461**, 393-398 (2009).
56. J. Win *et al.*, Sequence divergent RXLR effectors share a structural fold conserved across plant pathogenic oomycete species. *PLoS pathogens* **8**, (2012).
57. L. S. Boutemy *et al.*, Structures of Phytophthora RXLR effector proteins: a conserved but adaptable fold underpins functional diversity. *J Biol Chem* **286**, 35834-35842 (2011).
58. S. Wawra *et al.*, Host-targeting protein 1 (SpHtp1) from the oomycete Saprolegnia parasitica translocates specifically into fish cells in a tyrosine-O-sulphate-dependent manner. *Proceedings of the National Academy of Sciences of the United States of America* **109**, 2096-2101 (2012).
59. F. Trusch *et al.*, Cell entry of a host-targeting protein of oomycetes requires gp96. *Nature Communications* **9**, 2347 (2018).
60. R. Stam *et al.*, Identification and Characterisation CRN Effectors in Phytophthora capsici Shows Modularity and Functional Diversity. *PLOS ONE* **8**, e59517 (2013).
61. M. G. Links *et al.*, De novo sequence assembly of Albugo candida reveals a small genome relative to other biotrophic oomycetes. *BMC Genomics* **12**, 503 (2011).
62. A. J. E. Pelgrom *et al.*, Recognition of lettuce downy mildew effector BLR38 in Lactuca serriola LS102 requires two unlinked loci. *Molecular Plant Pathology* **0**, (2018).
63. A. K. J. Giesbers *et al.*, Effector-mediated discovery of a novel resistance gene against Bremia lactucae in a nonhost lettuce species. *New Phytol*, (2017).
64. J. H. Stassen *et al.*, Specific in planta recognition of two GKLR proteins of the downy mildew Bremia lactucae revealed in a large effector screen in lettuce. *Molecular Plant-Microbe Interactions* **26**, 1259-1270 (2013).
65. A. M. V. Ah-Fong, K. S. Kim, H. S. Judelson, RNA-seq of life stages of the oomycete Phytophthora infestans reveals dynamic changes in metabolic, signal transduction, and pathogenesis genes and a major role for calcium signaling in development. *BMC Genomics* **18**, 198 (2017).
66. K. Yoshida *et al.*, The rise and fall of the Phytophthora infestans lineage that triggered the Irish potato famine. *eLife* **2**, e00731 (2013).
67. T. A. Klochkova, Y. J. Shin, K.-H. Moon, T. Motomura, G. H. Kim, New species of unicellular obligate parasite, Olpidiopsis pyropiae sp. nov., that plagues Pyropia sea farms in Korea. *Journal of Applied Phycology* **28**, 73-83 (2016).

68. L. Parra *et al.*, Rationalization of genes for resistance to Bremia lactucae in lettuce. *Euphytica* **210**, 309-326 (2016).
69. S. G. Kunjeti *et al.*, Detection and Quantification of Bremia lactucae by Spore Trapping and Quantitative PCR. *Phytopathology* **106**, 1426-1437 (2016).
70. S. Zhong *et al.*, High-throughput illumina strand-specific RNA sequencing library preparation. *Cold Spring Harbor protocols* **2011**, 940-949 (2011).
71. M. D. Bennett, I. J. Leitch, H. J. Price, J. S. Johnston, Comparisons with Caenorhabditis (~100 Mb) and Drosophila (~175 Mb) Using Flow Cytometry Show Genome Size in Arabidopsis to be ~157 Mb and thus ~25 % Larger than the Arabidopsis Genome Initiative Estimate of ~125 Mb. *Annals of Botany* **91**, 547-557 (2003).
72. E. W. Myers *et al.*, A Whole-Genome Assembly of *Drosophila*. *Science (New York, N.Y.)* **287**, 2196-2204 (2000).
73. M. Boetzer, C. V. Henkel, H. J. Jansen, D. Butler, W. Pirovano, Scaffolding pre-assembled contigs using SSPACE. *Bioinformatics* **27**, 578-579 (2011).
74. A. Bashir *et al.*, A hybrid approach for the automated finishing of bacterial genomes. *Nat Biotech* **30**, 701-707 (2012).
75. S. Huang, M. Kang, A. Xu, HaploMerger2: rebuilding both haploid sub-assemblies from high-heterozygosity diploid genome assembly. *Bioinformatics*, (2017).
76. M. Hunt *et al.*, REAPR: a universal tool for genome assembly evaluation. *Genome Biology* **14**, R47 (2013).
77. M. Boetzer, W. Pirovano, Toward almost closed genomes with GapFiller. *Genome Biology* **13**, R56 (2012).
78. D. Mapleson, G. Garcia Accinelli, G. Kettleborough, J. Wright, B. J. Clavijo, KAT: a K-mer analysis toolkit to quality control NGS datasets and genome assemblies. *Bioinformatics* **33**, 574-576 (2017).
79. C. Soderlund, W. Nelson, A. Shoemaker, A. Paterson, SyMAP: A system for discovering and viewing syntenic regions of FPC maps. *Genome Research* **16**, 1159-1168 (2006).
80. K. Katoh, D. M. Standley, MAFFT multiple sequence alignment software version 7: improvements in performance and usability. *Mol Biol Evol* **30**, (2013).
81. A. Stamatakis, RAxML version 8: a tool for phylogenetic analysis and post-analysis of large phylogenies. *Bioinformatics* **30**, 1312-1313 (2014).
82. H. Li, Aligning sequence reads, clone sequences and assembly contigs with BWA-MEM. *arXiv preprint arXiv:1303.3997*, (2013).
83. S. Reyes-Chin-Wo *et al.*, Genome assembly with in vitro proximity ligation data and whole-genome triplication in lettuce. **8**, 14953 (2017).
84. M. G. Grabherr *et al.*, Trinity: reconstructing a full-length transcriptome without a genome from RNA-Seq data. *Nature biotechnology* **29**, 644-652 (2011).
85. B. J. Haas *et al.*, De novo transcript sequence reconstruction from RNA-Seq: reference generation and analysis with Trinity. *Nature protocols* **8**, 10.1038/nprot.2013.1084 (2013).
86. B. L. Cantarel *et al.*, MAKER: An easy-to-use annotation pipeline designed for emerging model organism genomes. *Genome Research* **18**, 188-196 (2008).
87. I. Korf, Gene finding in novel genomes. *BMC Bioinformatics* **5**, 59 (2004).
88. S. C. Whisson *et al.*, A translocation signal for delivery of oomycete effector proteins into host plant cells. *Nature* **450**, (2007).
89. S. M. Geib *et al.*, Genome Annotation Generator: a simple tool for generating and correcting WGS annotation tables for NCBI submission. *GigaScience* **7**, giy018-giy018 (2018).
90. A. R. Quinlan, BEDTools: the Swiss-army tool for genome feature analysis. *Current protocols in bioinformatics / editoral board, Andreas D. Baxevanis ... [et al.]* **47**, 11.12.11-11.12.34 (2014).
91. J. E. Stajich *et al.*, FungiDB: an integrated functional genomics database for fungi. *Nucleic Acids Research* **40**, D675-D681 (2012).

92. A. Smit, R. Hubley, *RepeatModeler Open-1.0.*, (2008-2015).
93. D. Ellinghaus, S. Kurtz, U. Willhoeft, LTRharvest, an efficient and flexible software for de novo detection of LTR retrotransposons. *BMC Bioinformatics* **9**, 18 (2008).
94. S. Steinbiss, U. Willhoeft, G. Gremme, S. Kurtz, Fine-grained annotation and classification of de novo predicted LTR retrotransposons. *Nucleic Acids Research* **37**, 7002-7013 (2009).
95. L. Derevnina *et al.*, Genome Sequence and Architecture of the Tobacco Downy Mildew Pathogen Peronospora tabacina. *Molecular Plant-Microbe Interactions* **28**, 1198-1215 (2015).
96. A. Smit, R. Hubley, P. Green, *RepeatMasker open-4.0.*, (2013-2015).
97. F. Sievers *et al.*, Fast, scalable generation of high-quality protein multiple sequence alignments using Clustal Omega. *Molecular Systems Biology* **7**, 539-539 (2011).
98. Z. Yang, PAML 4: Phylogenetic Analysis by Maximum Likelihood. *Molecular Biology and Evolution* **24**, 1586-1591 (2007).
99. R Development Core Team. (R Foundation for Statistical Computing, Vienna, Austria, 2012).
100. H. Wickham, *ggplot2: elegant graphics for data analysis*. (Springer, 2016).
101. R. Leinonen, H. Sugawara, M. Shumway, C. on behalf of the International Nucleotide Sequence Database, The Sequence Read Archive. *Nucleic Acids Research* **39**, D19-D21 (2011).
102. G. Marçais, C. Kingsford, A fast, lock-free approach for efficient parallel counting of occurrences of k-mers. *Bioinformatics* **27**, 764-770 (2011).
103. G. W. Vurture *et al.*, GenomeScope: fast reference-free genome profiling from short reads. *Bioinformatics* **33**, 2202-2204 (2017).
104. B. Bushnell, BBMap short read aligner. *University of California, Berkeley, California. URL* http://sourceforge.net/projects/bbmap, (2016).
105. H. Li *et al.*, The Sequence Alignment/Map format and SAMtools. *Bioinformatics* **25**, (2009).
106. H. Li, A statistical framework for SNP calling, mutation discovery, association mapping and population genetical parameter estimation from sequencing data. *Bioinformatics* **27**, 2987-2993 (2011).
107. P. Danecek *et al.*, The variant call format and VCFtools. *Bioinformatics* **27**, 2156-2158 (2011).
108. A. Manichaikul *et al.*, Robust relationship inference in genome-wide association studies. *Bioinformatics* **26**, 2867-2873 (2010).
109. L. Baxter *et al.*, Signatures of adaptation to obligate biotrophy in the Hyaloperonospora arabidopsidis genome. *Science (New York, N.Y.)* **330**, (2010).
110. Y. Dussert *et al.*, Draft genome sequence of Plasmopara viticola, the grapevine downy mildew pathogen. *Genome announcements* **4**, e00987-00916 (2016).
111. L. Yin *et al.*, Genome sequence of Plasmopara viticola and insight into the pathogenic mechanism. *Scientific Reports* **7**, (2017).
112. M. Kobayashi *et al.*, Genome analysis of the foxtail millet pathogen Sclerospora graminicola reveals the complex effector repertoire of graminicolous downy mildews. *BMC Genomics* **18**, 897 (2017).

743 **Figure Legends**

744 **Fig. 1. Genome and assembly features of *B. lactucae*.** a) Estimation of genome size of
745 heterokaryotic isolate C82P24 by flow cytometry. The nuclei of *B. lactucae* have two peaks calibrated
746 relative to the reference nuclei of *Oryza sativa* (2C = 867 Mb). Nuclei of isolate C82P24 were
747 estimated to be 305 Mb (2C) and 599 Mb (4C). Another 38 isolates all have similar sizes
748 (Supplementary Table 1). b) Extensive collinearity between *B. lactucae* and *P. sojae* displayed as a
749 SyMap plot. c) Comparison of heterozygosity in 54 isolates of 22 oomycete species (Supplementary
750 Table 8). d) High quality of *B. lactucae* assembly demonstrated by inclusion of k-mers from paired-
751 end reads in the assembly. Colors indicate presence of k-mers in the assembly, relative to reads.
752 Black: the distribution of k-mers present in the read set but absent in the assembly. Red: K-mers
753 present in the read set and once in the assembly. Purple: K-mers present in the reads set and twice
754 in the assembly. The first peak depicts heterozygous k-mers and the second peak depicts
755 homozygous k-mers. A high-quality consensus assembly will contain half the k-mers in the first peak,
756 the other half of which should be black due to heterozygosity, and all the k-mers in the second peak
757 should be present only once, which therefore should be red. Very few duplicated k-mers were
758 detected in the SF5 assembly. K-mers derived from repeat sequences have higher multiplicity and
759 are not shown.

760 **Fig. 2. Comparative LTR-RT analysis.** a) Comparison of ages of LTR elements in 15 oomycete
761 assemblies. Distribution of percent divergence of LTR elements is shown for 12 downy mildew (*B.*
762 *lactcuae*, *H. arabidopsidis*, *P. effusa*, *P. tabacina*, *P. viticola,* and *S. graminicola*) and three
763 *Phytophthora* (*P. infestans*, *P. ramorum,* and *P. sojae*) assemblies. Statistics of these assemblies are
764 included in Table 1. LTR elements of *B. lactucae* are younger than elements in other downy mildew
765 assemblies. b) Counts of unique LTR-RTs harvested and annotated from each genome surveyed.
766 Larger assemblies (Table 1) are observed as having higher counts of LTR-RTs. Bars are ordered by the
767 percent of the genome masked displayed in panel c. Only partial and no full elements could be found

768 for *P. halstedii*. c) Scatterplot demonstrating the percentage of the assembly sequence that is
769 masked by annotated LTR-RTs and partial elements. Colors and order are retained from panel b. The
770 percentage of the assembly masked increases with assembly size. *B. lactucae* is an outlier as it has a
771 medium assembly size, but the highest masked percentage.

772 **Fig. 3. Polyphyly of downy mildews and paraphyly of *Phytophthora* spp.** Phylogenetic maximum
773 likelihood tree based on the analysis of 18 BUSCO proteins across 29 Peronosporaceae species
774 rooted with *Pythium ultimum* as the outgroup. The 20 *Phytothphora* species were selected to
775 represent the nine published *Phytophthora* clades indicated by the number in brackets. Downy
776 mildew clades 1 and 2 are shown in red and blue, respectively. Support for nodes is shown as
777 percent bootstrap values from 1,000 iterations. Scale is the mean number of amino acid
778 substitutions per site.

779 **Fig. 4. Heterokaryosis in *B. lactucae*.** Example alternative allele frequency plots of SNPs detected in
780 four field isolates of *B. lactucae.* A) A unimodal distribution with a 1:1 ratio of reads supporting
781 alternative and reference alleles seen in the homokaryotic SF5 isolate. B) A trimodal distribution
782 with peaks at 1:1, 1:3, and 3:1 ratios of reads supporting alternate alleles in the heterokaryotic
783 C82P24 isolate, consistent with two nuclei being present in equal proportions. C) A bimodal
784 distribution with two peaks at 1:2 and 2:1 ratios of reads supporting alternative alleles observed in
785 the heterokaryotic isolate C041017, consistent with three nuclei being present in equal proportions.
786 D) The complex distribution observed in isolate C90D33, consistent with an uneven mixture of
787 multiple nuclei in a heterokaryotic isolate. Allele distributions of 31 isolates are shown in
788 Supplementary Fig. 4.

789 **Fig. 5. The presence of two half-sib groups in sexual progeny derived from a cross between a**
790 **homokaryotic and a heterokaryotic isolate.** Kinship analysis based on SNPs segregating in sexual
791 progeny generated by crossing SF5 (homokaryotic) with C82P24 (heterokaryotic). The first square
792 delineates the majority of the offspring as one group of siblings derived from the same two parental

nuclei (homokaryon 1, HK1). The second square delineates the remaining offspring as a second group of siblings derived from a different nucleus in C82P24 (homokaryon2, HK2). Relatedness of these two groups is consistent with having one parental nucleus in common derived from SF5. Relatedness of single-spore asexual derivatives of both isolates is also shown. Single-spore derivatives of C82P24 had a high relatedness to all other C82P24 derivatives and the original isolate. These derivatives and C82P24 were equidistant to all offspring, indicating that both nuclei in the heterokaryon contributed to the offspring and that the heterokaryotic C82P24 isolate had not been separated into homokaryotic components by generating single-spore derivatives.

Fig. 6. Genomic and phenotypic instability of the heterokaryotic isolate C98O622b. (i) Relatedness analysis of ten asexual single-spore derivatives of C98O622b placed them into three genomic groups. One group of derivatives, A to F, were heterokaryotic and highly similar to C98O622b. The other two groups, derivatives G to I and derivative J, were each homokaryotic, less similar to C98O622b than the heterokaryotic group was, and even less similar to each other. Combining reads *in silico* of isolates G to I did not change their relatedness to other isolates; combining reads of any of G to I with J scored similarly high in relatedness to C98O622b as derivatives A to F. (ii) Phenotypic differences between heterokaryotic and homokaryotic derivatives of C98O622b compared to the original isolate. Derivatives A to F were virulent on both *Dm4* and *Dm15*; however, derivatives G to I were avirulent on *Dm4* and virulent on *Dm15*, while derivative J showed the reverse virulence phenotype. (iii) Alternative allele frequency plots of four C98O622b derivatives showing that derivatives A to F are heterokaryotic and G to J are homokaryotic. Alternative allele frequency plots of the derivatives A, D to G, and I are shown in Supplementary Fig. 7. (iv) Alternative allele frequency plots of heterokaryotic derivatives based only on SNPs unique to each homokaryotic derivative. In a balanced heterokaryon such as derivative B, SNPs unique to each homokaryon are observed at frequencies of 0.25 and 0.75, consistent with the presence of each nucleus in a 1:1 ratio. In an unbalanced heterokaryon, such as derivative C, SNPs unique to homokaryotic derivatives G, H, and I are present at frequencies of approximately 0.17 and 0.83, while SNPs unique to derivative J are

819 present at frequencies of 0.33 and 0.66; this is consistent with twice as many nuclei of J as those of
820 G, H, and I. Similar distributions are observed for derivatives A, D, and E, indicating that they are
821 unbalanced heterokaryons (Supplementary Figure 8).

822 **Fig. 7. Differences in fitness between heterokaryotic and homokaryotic derivatives of C98O622b.**
823 A) Growth of four single-spore derivatives on the universally susceptible lettuce cv. Green Towers
824 (n=16). Heterokaryons exhibit higher growth mass per lettuce seedling and DNA quantity collected
825 per mL of sporangia suspension. Area under the curve measurements demonstrate significantly
826 faster sporulation of heterokaryon derivative B compared to homokaryon derivative I. B) Growth
827 curves of heterokaryotic isolates (black lines) versus homokaryotic isolates (red lines) on differential
828 lettuce lines NunDM15 (*Dm15*) and R4T57D (*Dm4*), demonstrating that viable homokaryons
829 sporulate faster on selective hosts than heterokaryons (n=10).

830 **Fig. 8. The multinucleate architecture of *B. lactucae*.** Lettuce cotyledons infected with *B. lactucae*
831 stained with 4',6-diamidino-2-phenylindole (DAPI) to render nuclear DNA fluorescent. A) Densely
832 multinucleate coenocytic mycelium growing between spongy mesophyll cells of a non-transgenic
833 lettuce cotyledon five days post infection (dpi), prior to sporulation. Two of six multinucleate
834 haustoria that have invaginated the host plasmalemma are indicated (h). The larger plant nuclei
835 fluoresce magenta. Autofluorescent chloroplasts are visualized as green. B) Infected lettuce
836 cotyledon stably expressing DsRED stained seven dpi at the onset of sporulation. The multinucleate
837 stem of a sporangiophore is visible exiting a stoma. Two multinucleate spores are visible on the
838 cotyledon surface (arrowed). Small DAPI-stained bacterial cells are also visible.

839

840 Table 1. Comparative statistics of downy mildew genome assemblies and select *Phytophthora* assemblies.

841

Genus	Species	Isolate/label	Scaffold N50 (kb) [a]	Scaffold Count	Contig N50 (kb)	Contig Count	Assembly size (Mb)	Gaps (%)	Gene model count [b]	BUSCO Complete (%)	BUSCO Duplicated (%)	BUSCO Fragmented (%)	BUSCO Missing (%)	Reference
Bremia	*lactucae*	SF5	**6116**	122	30	4997	115.9	21.482	9781	98.3	3.4	0.9	0.8	This study
Hyaloperonospora	*arabidopsidis*	Cala2	24	9283	22	9658	70.3	0.016	n/a	96.6	1.3	3	0.4	n/a
		Emoy2	332	3044	43	10401	78.9	10.224	14321	96.6	4.7	2.6	0.8	(*109*)
		Noks1	19	12086	18	13094	74.2	0.025	n/a	97	1.3	3	0	n/a
Peronospora	*effusa*	R13	72	784	48	1472	32.2	0.261	8607	97.8	0.4	0	2.2	(*47*)
		R14	61	880	52	1275	30.8	0.564	8571	97	0	0.4	2.6	
	tabacina	968-J2	79	4016	11	10799	63.1	27.351	11310	94.9	29.5	3	2.1	(*95*)
		968-S26	61	3245	15	8552	55.3	19.089	10707	94.9	29.1	3.4	1.7	
Plasmopara	*halstedii*	Ph8-99-BlA4	**1546**	3162	16	25359	75.3	11.322	15469	97.4	0	1.7	0.9	(*48*)
	viticola	INRA-PV221	181	1883	49	3995	74.7	2.83	n/a	95.7	4.7	1.7	2.6	(*110*)
		JL-7-2	172	2165	14	23193	101.2	16.712	n/a (17014)	84.6	8.1	8.5	6.9	(*111*)
Pseudoperonospora	*cubensis*	ASM25260v1	4	35539	4	35539	64.3	0	n/a	92.8	0.9	6.4	0.8	(*112*)
Phytophthora	*infestans*	T30-4	**1589**	4921	44	18288	228.5	16.806	17797	97	3	1.3	1.7	(*55*)
	ramorum	ASM14973v1	308	2576	48	7589	66.7	18.346	15605	97.4	3	1.7	0.9	(*45*)
	sojae	Physo3	**7609**	83	386	863	82.6	3.959	26489	99.5	3.8	0	0.5	(*45*)

842 [a] Bold numbers indicated scaffold N_{50}'s over 1 Mb

843 [b] n/a indicates that annotations could not be found or weren't described. Bracketed numbers indicate reported numbers from paper.

844

Table 2. Repeat statistics of the *B. lactucae* assembly.

	Number of elements	Total length (bp)	Percentage of contig sequence
Long terminal repeat elements	63,720	61,227,642	67.3%
Copia	5,659	6,314,733	6.9%
Gypsy	57,655	53,338,585	58.6%
Short interspersed nuclear element	35	15,270	0.02%
Long interspersed nuclear repeat	182	471,735	0.52%
DNA elements	337	471,455	0.52%
Unclassified	685	1,050,820	1.15%

854 Table 3. Counts of annotated effectors in the *B. lactucae* assembly.

855

	Genome	Transcriptome*
RxLR	36	27
[GHQ]xLR	31	20
RxL[GKQ]	30	27
RxLR - EER	22	13
[GHQ]xLR -EER	18	8
RxL[GKQ] -EER	11	4
RxLR-WY	2	1
RxL[GKQ]-WY	2	2
RxLR - EER - WY	6	6
[GHQ]xLR -EER - WY	1	1
SP - WY	26	19
WY	19	13
SP - CRN	2	0
CRN	74	6

*Presence in transcriptome inferred by tBLASTn

Total proteins with RxLR	66
Total proteins with degenerate RxLR	95
Total proteins with WY domain	56
Total Crinklers	76

856

Figure 1

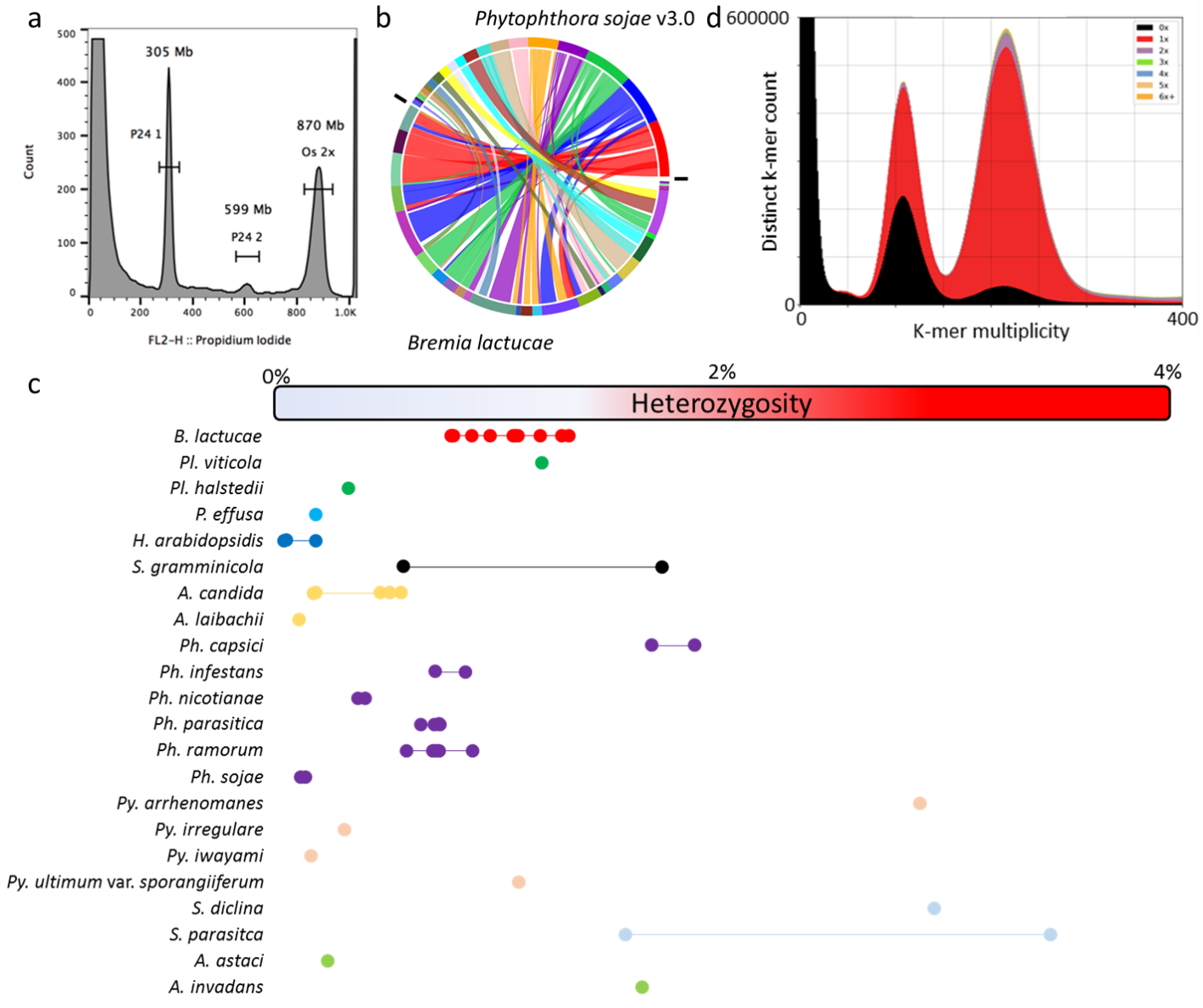
a
305 Mb
P24 1
870 Mb
Os 2x
599 Mb
P24 2
Count
FL2-H :: Propidium Iodide
b
Phytophthora sojae v3.0
Bremia lactucae
d
Distinct k-mer count
K-mer multiplicity
0x
1x
2x
3x
4x
5x
6x+
c
0%
2%
4%
Heterozygosity
B. lactucae
Pl. viticola
Pl. halstedii
P. effusa
H. arabidopsidis
S. gramminicola
A. candida
A. laibachii
Ph. capsici
Ph. infestans
Ph. nicotianae
Ph. parasitica
Ph. ramorum
Ph. sojae
Py. arrhenomanes
Py. irregulare
Py. iwayami
Py. ultimum var. sporangiiferum
S. diclina
S. parasitca
A. astaci
A. invadans

Figure 2

Figure legend here.

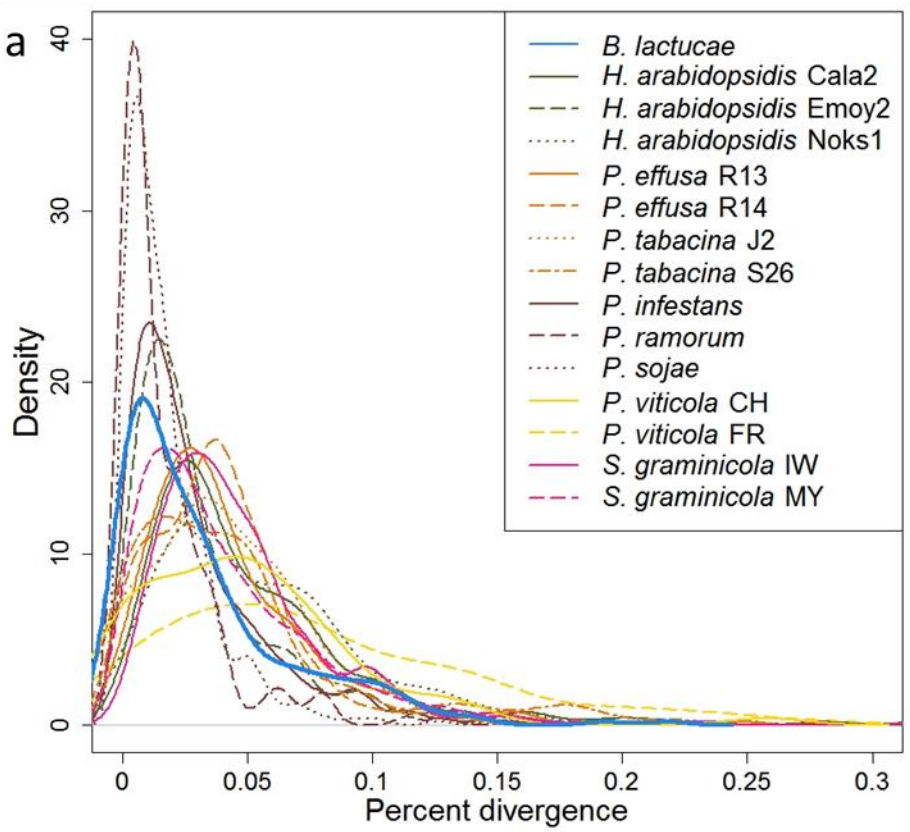

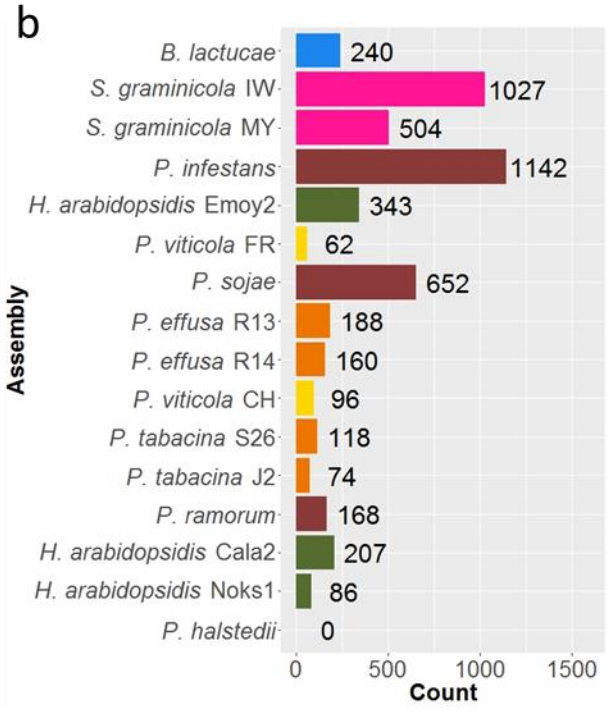

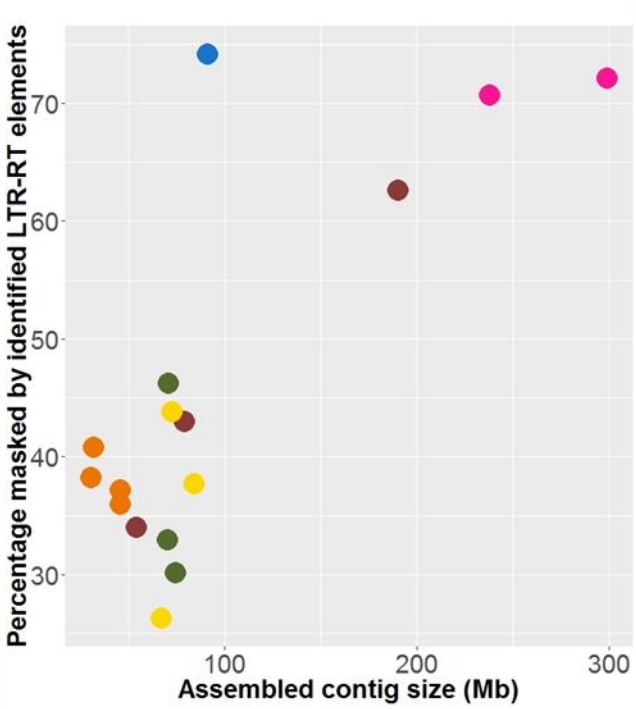

Figure 3

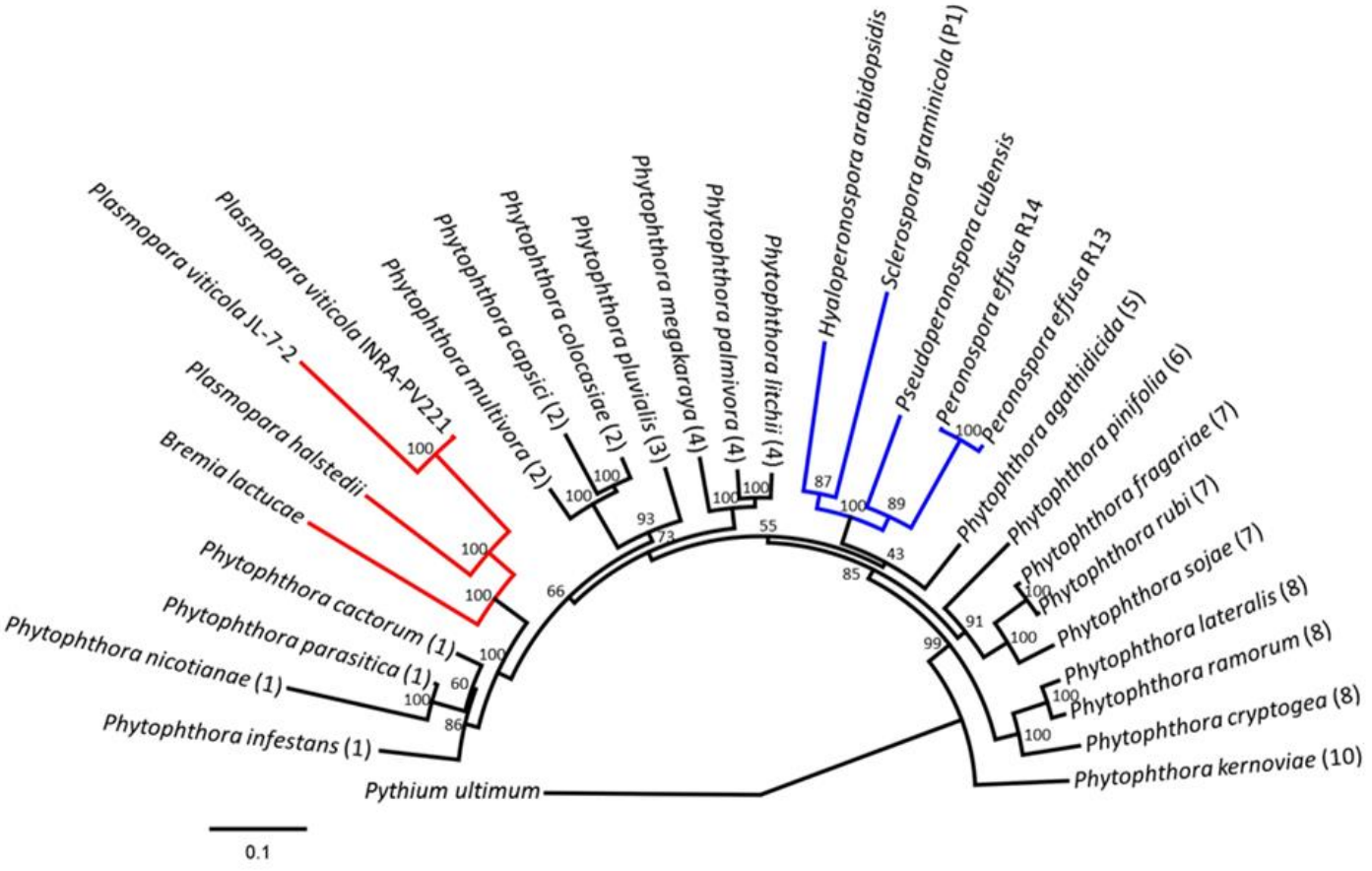
Plasmopara viticola JL-7-2
Plasmopara viticola INRA-PV221
Plasmopara halstedii
Bremia lactucae
Phytophthora cactorum (1)
Phytophthora parasitica (1)
Phytophthora nicotianae (1)
Phytophthora infestans (1)
Pythium ultimum
Phytophthora multivora (2)
Phytophthora capsici (2)
Phytophthora colocasiae (2)
Phytophthora pluvialis (3)
Phytophthora megakaraya (4)
Phytophthora palmivora (4)
Phytophthora litchii (4)
Hyaloperonospora arabidopsidis
Sclerospora graminicola (P1)
Pseudoperonospora cubensis
Peronospora effusa R14
Peronospora effusa R13
Phytophthora agathidicida (5)
Phytophthora pinifolia (6)
Phytophthora fragariae (7)
Phytophthora rubi (7)
Phytophthora sojae (7)
Phytophthora lateralis (8)
Phytophthora ramorum (8)
Phytophthora cryptogea (8)
Phytophthora kernoviae (10)
0.1

Figure 4

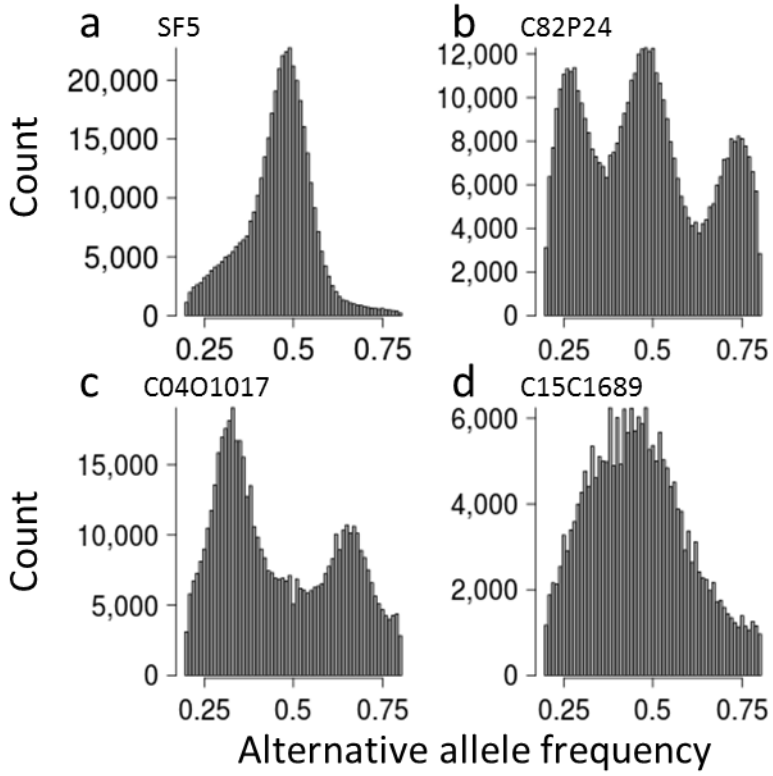
a
SF5
b
C82P24
c
C04O1017
d
C15C1689
Count
Count
20,000
15,000
10,000
5,000
0
12,000
8,000
6,000
4,000
2,000
0.25
0.5
0.75
Alternative allele frequency

Figure 5

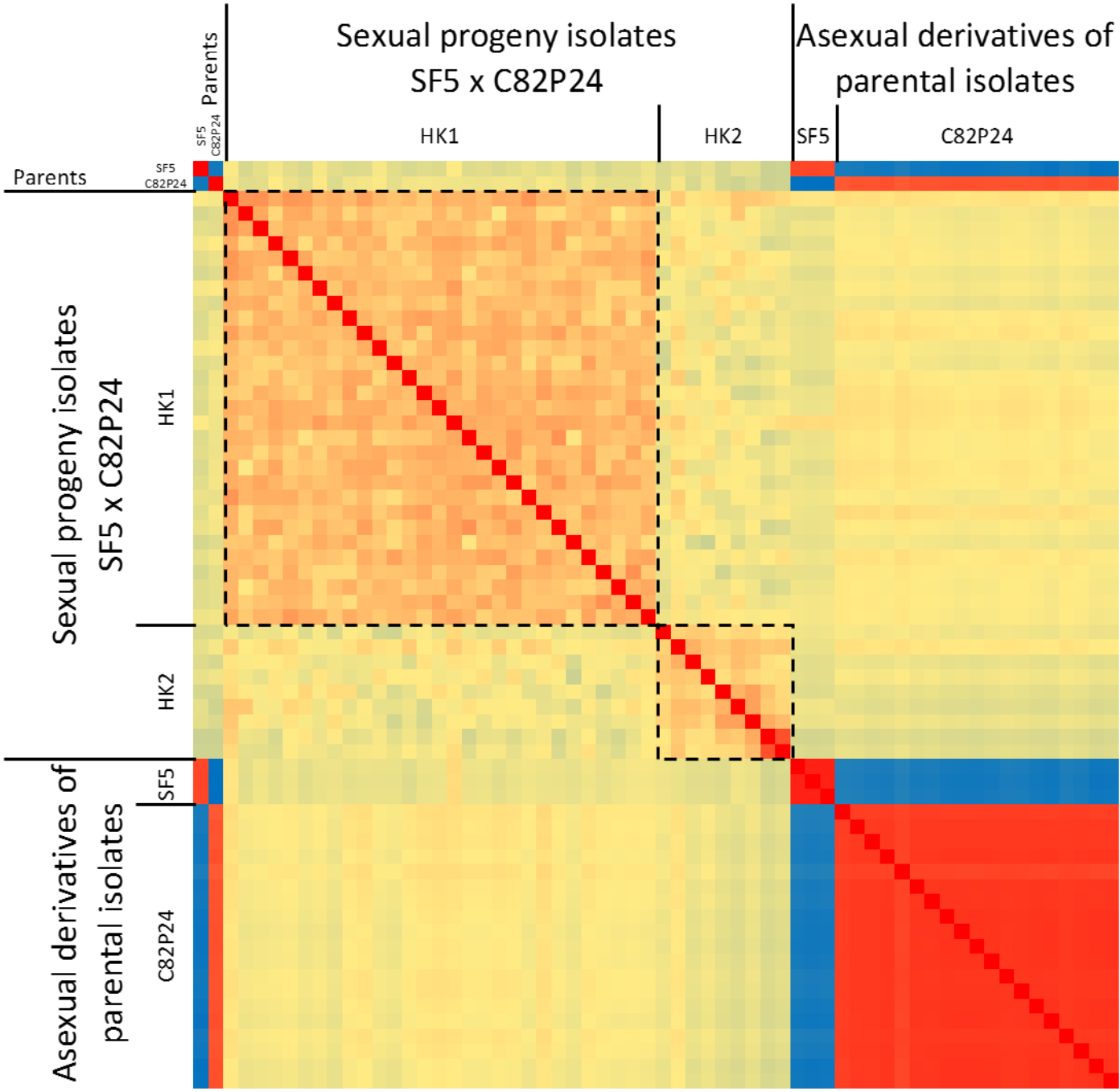
Parents
Sexual progeny isolates
SF5 x C82P24
Asexual derivatives of
parental isolates
SF5
C82P24
HK1
HK2
SF5
C82P24
Parents
Sexual progeny isolates
SF5 x C82P24
HK1
HK2
Asexual derivatives of
parental isolates
SF5
C82P24

Figure 6

i)

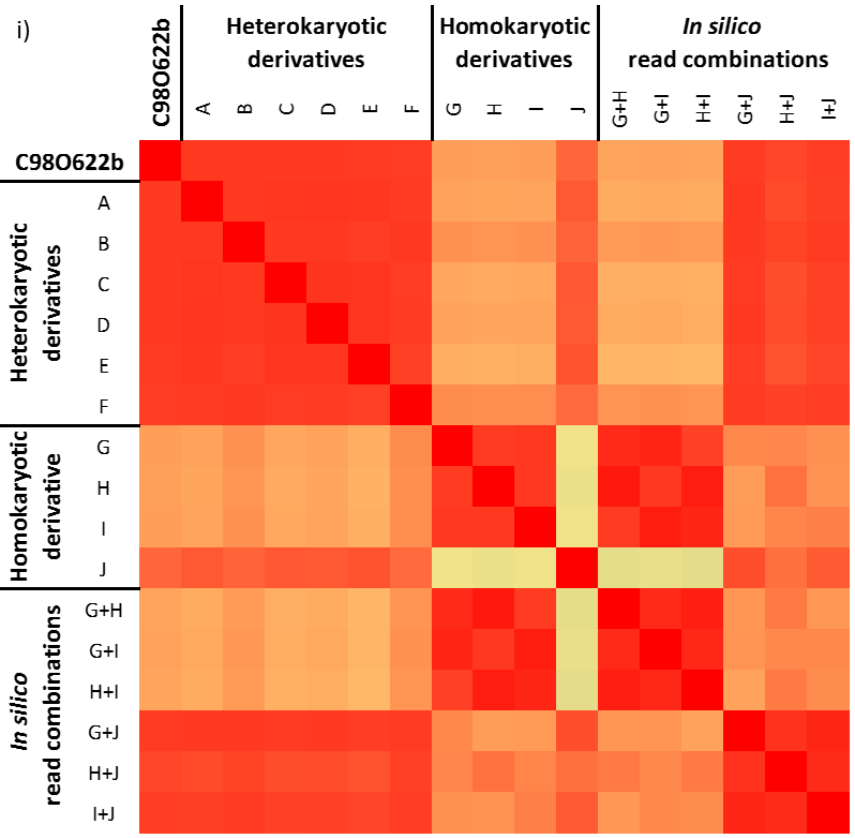

iii)

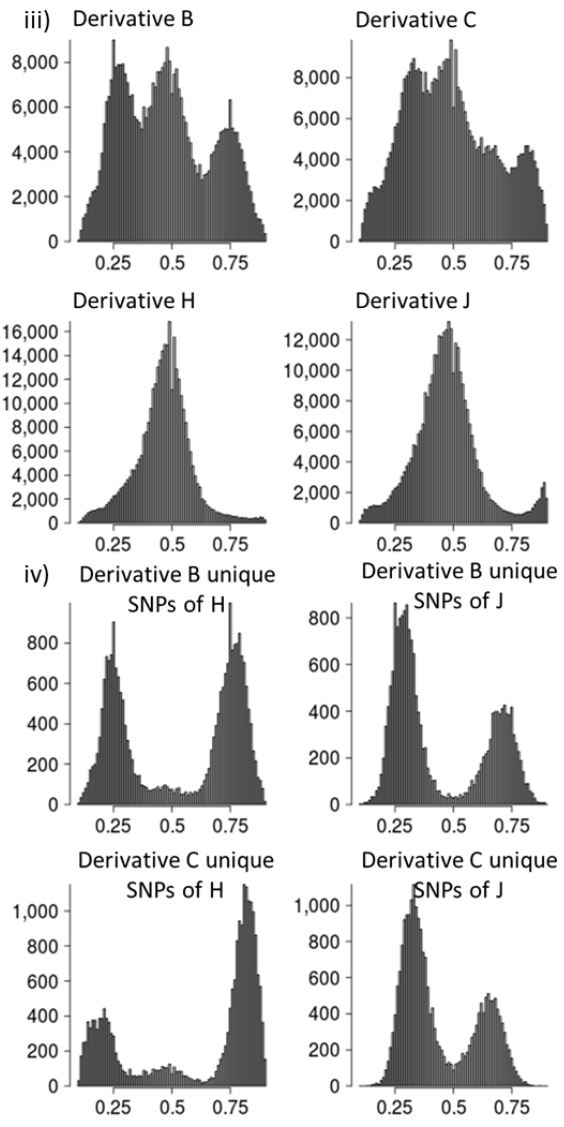

ii)

C98O622b	*Dm* gene 4	15
Original isolate	+	+
Derivatives A to F	+	+
Derivatives G to I	-	+
Derivative J	+	-

Figure 7

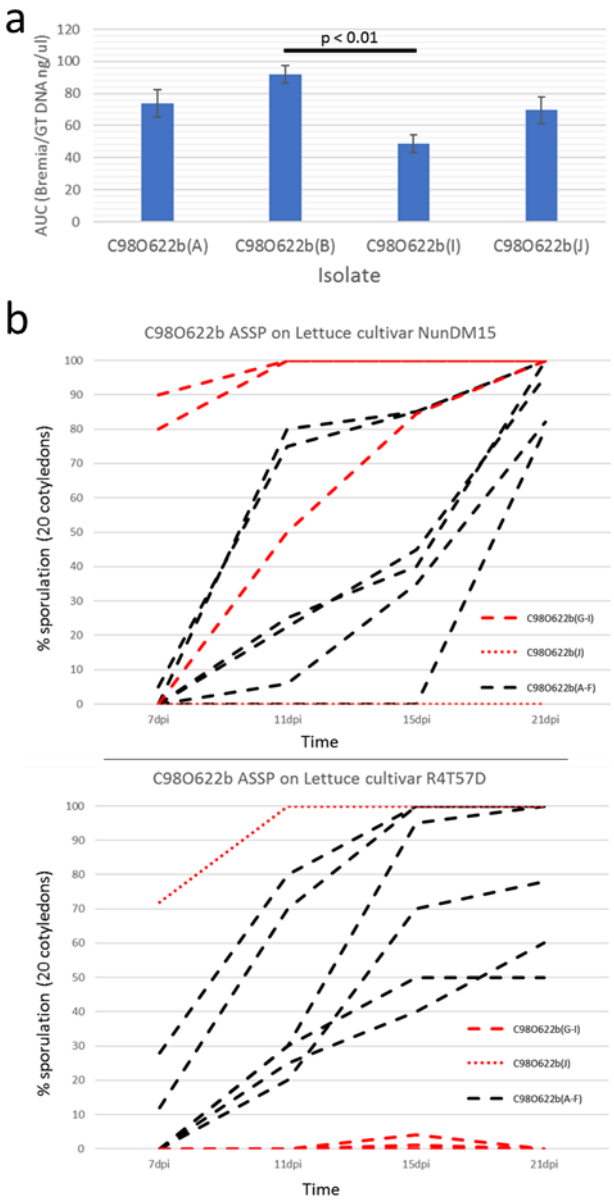
a
AUC (Bremia/GT DNA ng/ul)
p < 0.01
C98O622b(A)
C98O622b(B)
C98O622b(I)
C98O622b(J)
Isolate
b
C98O622b ASSP on Lettuce cultivar NunDM15
% sporulation (20 cotyledons)
C98O622b(G-I)
C98O622b(J)
C98O622b(A-F)
7dpi
11dpi
15dpi
21dpi
Time
C98O622b ASSP on Lettuce cultivar R4T57D
% sporulation (20 cotyledons)
C98O622b(G-I)
C98O622b(J)
C98O622b(A-F)
7dpi
11dpi
15dpi
21dpi
Time

Figure 8